Toxicology 420 (2019) 1–10

Contents lists available at ScienceDirect

Toxicology

journal homepage: www.elsevier.com/locate/toxicol

Investigating the *in vitro* metabolism of the dental resin monomers BisGMA, BisPMA, TCD-DI-HEA and UDMA using human liver microsomes and quadrupole time of flight mass spectrometry

Philippe Vervliet[a,*], Jens Van Den Plas[a], Siemon De Nys[b], Radu Corneliu Duca[c], Imke Boonen[d], Marc Elskens[d], Kirsten L. Van Landuyt[b], Adrian Covaci[a,*]

[a] Toxicological Centre, University of Antwerp, Universiteitsplein 1, 2610, Wilrijk, Belgium
[b] KU Leuven (University of Leuven), Department of Oral Health Sciences, BIOMAT & University Hospitals Leuven (UZ Leuven), Dentistry, Leuven, Belgium
[c] Environment and Health, Department of Public Health and Primary Care, KU Leuven, Kapucijnenvoer 35, 3000, Leuven, Belgium
[d] Department of Analytical, Environmental and Geo-Chemistry, Vrije Universiteit Brussel, Pleinlaan 2, 1050, Ixelles, Belgium

ARTICLE INFO

Keywords:
In vitro biotransformation
Human liver microsomes
Cytosolic fractions
Liquid chromatography-mass spectrometry
Dental resins

ABSTRACT

Dental resin systems have been in use for several decades. (Meth)acrylic monomers are an important part of the matrix system and are either based on BPA while others lack the BPA core. The degree of conversion during restoration is in general between 50–70 % allowing leaching from unreacted monomers to the oral cavity where they can be taken up through the pulp or gastrointestinal tract after ingestion with subsequent hepatic metabolism. This study identified the *in vitro* Phase I and Phase II metabolism of the dental resin monomers BisGMA, UDMA, BisPMA and TCD-DI-HEA, using human liver microsomes (HLM) and human liver cytosols. During Phase I incubation with HLM, the (meth)acrylic acid in the monomers was rapidly removed followed by oxidative and hydroxylation pathways. For BisPMA an O-dealkylation pathway occurred resulting in the formation of BPA. The carbamates present in TCD-DI-HEA and UDMA were resistant to biotransformation reactions. Phase II biotransformation products were only observed for BisPMA and included conjugation reactions with sulphate and glucuronic acid. In total 4, 3, 12 and 3 biotransformation products were identified in this study for BisGMA, UDMA, BisPMA and TCD-DI-HEA respectively. Possible human health effects of these biotransformation products remain unclear due to limited data availability.

1. Introduction

Dental resins systems have been in use for dental restorations for several decades (Forss and Widström, 2001; Khalaf et al., 2014; Sunnegardh-Gronberg et al., 2009) and have gained an even higher market share after the Minamata convention and the encouragement of the World Health Organization (WHO) for a global phase-down of dental amalgam (Lynch and Wilson, 2013; United Nations Environment Programme, 2013; World Health Organisation, 2011). Next to inorganic fillers, the resin matrix consists of (meth)acrylic monomers which can be self-cured, light-cured or a combination of both techniques. Commonly used monomers are either based on bisphenol A (BPA), such as Bisphenol A glycidyl methacrylate (BisGMA) and Bisphenol A dimethacrylate (BisDMA). Others lack the BPA backbone and include triethylene glycol dimethacrylate (TEGDMA) and urethane dimethacrylate (UDMA). As with the amalgam systems, the safety of the resin monomer systems is also under investigation (Söderholm and Mariotti, 1999). BPA, serving as a backbone for several monomers, has been widely studied and is a known endocrine disrupting compound (EDC) with estrogenic effects (Maffini et al., 2006; Rochester, 2013; Rubin, 2011). Next to BPA, several studies have investigated the effects of the dental monomers. Estrogenic effects have been reported for BisDMA, but not for BisGMA (Bonefeld-Jørgensen et al., 2007; Olea et al., 1996; Tarumi et al., 2000). However, high doses of BisGMA were associated with an increased uterine wet weight and uterine collagen content in ovariectomized mice as well as a reduced fertility in male mice (Al-Hiyasat and Darmani, 2006; Mariotti et al., 1998).

Upon restoration, the degree of conversion (DC) is in general between 50–70 % allowing leaching of remaining monomers from the polymer matrix to the oral cavity where they can migrate through the dentine to the pulp, resulting in a systemic uptake (Lempel et al., 2014; Pongprueksa et al., 2015). Secondly, monomers can be ingested by the

* Corresponding authors.
E-mail addresses: philippe.vervliet@uantwerpen.be (P. Vervliet), adrian.covaci@uantwerpen.be (A. Covaci).

https://doi.org/10.1016/j.tox.2019.03.007
Received 30 December 2018; Received in revised form 16 March 2019; Accepted 20 March 2019
Available online 29 March 2019
0300-483X/

patient with subsequent hepatic metabolism after an uptake through the gastrointestinal tract (Gupta et al., 2012; Reichl et al., 2008; Van Landuyt et al., 2011).

Next to the effects of the parent molecules, (hydroxylated) metabolites can interfere with hormone action in tissues where they are generated or interact with hormone receptors in a tissue-specific manner (Zoeller et al., 2012). Burmaster et al and Kostoryz et al have previously investigated the *in vitro* stability, metabolism and biocompatibility of BisGMA. BisGMA was stable *in vitro* in aqueous conditions but rat plasma rapidly hydrolysed the BisGMA ester monomer to the tetrahydroxy metabolite (Burmaster et al., 2002). 90% of initial BisGMA disappeared after 10 min of incubation in hepatic S9 fractions and the tetrahydroxy metabolite bisphenol A bis(2,3-dihydroxypropyl) ether was identified. No other metabolites nor BPA were detected (Kostoryz et al., 2003). The smaller methacrylates used in dental resins 2-hydroxyethyl methacrylate (HEMA) and triethyleneglycol dimethacrylate (TEGDMA), have been previously investigated in an *in vivo* setting using guinea pigs or mice and have identified metabolic pathways with CO_2 as end product to be the main excretion of these monomers (Durner et al., 2009; Reichl et al., 2001, 2002).

So far BisDMA is the only known monomer to metabolize to BPA as this can rapidly occur by exposure to esterases (Burmaster et al., 2002) but this monomer is no longer commonly used. Kostoryz et al incubated BisGMA in liver S9 fractions but the authors reported this did not led to the formation of BPA (Kostoryz et al., 2003). Higher levels of BPA detected in saliva and urine after dental restorations thus originate from residual BPA present in the materials upon production (Joskow et al., 2006; Kingman et al., 2012; Kloukos et al., 2013; Maserejian et al., 2016; McKinney et al., 2014).

The present study aimed to identify Phase I and Phase II *in vitro* biotransformation products of BisGMA, 2,2-bis-(4-(3-methacryloxypropoxy)phenyl)propane (BisPMA), Bis-(acryloyloxymethyl)tricyclo [5.2.1.0.sup.2,6] decane (TCD-DI-HEA) and UDMA in order to propose potential, reliable and specific biomarkers for the detection in biomonitoring studies after dental restorations with dental materials containing these monomers. A recent study investigated the use of monomers in composite resins and found BisGMA and UDMA in 75% and 52% of investigated resins (Dursun et al., 2016). BisPMA and TCD-DI-HEA are less used proprietary alternatives.

The monomers were incubated with human liver microsomes (HLMs), human liver cytosols (HLCYTs) and appropriate cofactors to simulate the biotransformation reactions. Identification and elucidation of the biotransformation products formed in the *in vitro* assay was performed by analysing the samples using liquid chromatography coupled to accurate-mass quadrupole-time-of-flight mass spectrometry (LC-QTOF-MS) with a subsequent suspect screening data analysis workflow.

The present study focused on microsomal phase I metabolism and glucuronidation as well as sulfation by cytosolic enzymes. Pooled human liver microsomes (HLMs) are a suitable source of enzymes for examining *in vitro* human metabolism as they contain the major drug-metabolizing enzymes: the cytochrome P450 s (CYPs) and UDP-glucuronosyltransferases (UGTs) (Brandon et al., 2003; Fisher et al., 2000; Knights et al., 2016; Richter et al., 2017a). They are a cheap, quick and easy option for elucidating potential targets for toxicological screening (Hewitt et al., 2001; Richter et al., 2017b). Complementary to HLMs, human liver cytosol (HLCYT) contains sulfotransferase (SULT) and can be used to study *in vitro* sulfation reactions.

2. Materials and methods

2.1. Chemicals and reagents

HLMs (mixed gender, n = 50) were acquired from Tebu-Bio (Boechout, BE). HLCYT (mixed gender, n = 150), theophylline (anhydrous, > 99%), 2,5-uridinediphosphate glucuronic acid (UDPGA), adenosine-3′-phosphate 5′-phosphosulfate (PAPS, > 60%) lithium salt hydrate, alamethicin (neat, > 98%), dimethyl sulfoxide (DMSO), 4-nitrophenol (4-NP) and the analytical standard of BPA were obtained from Sigma-Aldrich (Missouri, US). NADPH tetrasodium salt hydrate (> 96%) was purchased from Acros (Geel, BE). Acetonitrile (ACN, HPLC-grade) and methanol (MeOH, ≥ 99.9% LC–MS grade) were acquired from Fisher Chemical (Loughborough, GB), formic acid (> 98%) and hydrochloric acid (37%) from Merck KGaA (Darmstadt, DE). A 100 mM TRIS-buffer was prepared by dissolving 12.11 g Trizma base (Janssen Chimica, Beerse, BE) and 1.02 g $MgCl_2$ (Merck KGaA, Darmstadt, DE) in 1 L ultrapure water. The pH was adjusted to 7.4 by adding 1 M HCl solution. Ultra-pure water was produced in-house with a PURELAB-purifier system of Elga Labwater (Tienen, BE). UDMA (CAS 72869-86-4) and BisGMA (CAS 1565-94-2) were received from Esstech Inc (Essington, PA, United States). TCD-DI-HEA (CAS 861437-11-8) was kindly provided by Heraeus Kulzer Benelux (Hanau, Germany). BisPMA was provided by 3 M (Seefeld, Germany).

2.2. In vitro metabolism assay metabolism assay

This study employed the *in vitro* assay optimized and used in previous studies (Ballesteros-Gomez et al., 2015; Erratico et al., 2016; Lai et al., 2015; Negreira et al., 2015; Vervliet et al., 2018b). An overview of the experimental setup can be found in the Supporting Information (Figure SI-1). All tested sample sets contained three replicates.

2.2.1. Phase I incubations

Phase I biotransformation products were generated using pooled HLMs. A reaction mixture containing 945 µL of TRIS-buffer (pH 7.4, 100 mM), 25 µL of HLMs (20 mg/mL in 250 mM sucrose in water) and 10 µL of monomer stock solution (0.5 mM in MeOH) was incubated in a 1.5 mL Eppendorf tube at 37 °C. 10 µL of NADPH (0.1 M in TRIS-buffer) was added after 5, 60 and 120 min to replenish NADPH levels. During incubation the total volume of organic solvent did not exceed 1% in order to avoid any effects on the microsomal activity (Jia and Liu, 2007). Three negative control samples (without parent compound, HLMs or NADPH) were prepared in parallel. The reaction was stopped after one or three hours by the addition of 250 µL ice-cold ACN containing 1% formic acid (phase I experiments) or by putting the samples on ice for 3 min (samples for further phase II experiments). The internal standard, theophylline, was prepared in the ice-cold ACN with 1% formic acid at 5 µg/mL. A positive control for phase I experiments was included by incubating 10 µL phenacetin (5 µg/mL in ultrapure water). The formation of two phase I biotransformation products - N-(4-hydroxyphenyl)-acetamide (P1) and N-(4-ethoxy-2-hydroxyphenyl)-acetamide (P2) was monitored.

2.2.2. Phase II incubations

Following the phase I experiments, samples were exposed to phase II conjugation through glucuronidation (GLU) and sulfation (SUL). For the GLU samples, 935 µL of the supernatant originating from the phase I samples was incubated with 25 µL of HLMs and 10 µL of alamethicin (1 mg/mL in DMSO). 10 µL of UDPGA (100 mM in TRIS-buffer) was added after 5, 60 and 120 min. SUL samples consisted of a mixture of 965 µL supernatant and 25 µL cytosol (20 mg/mL in buffer containing 150 mM potassium chloride and 50 mM Tris, pH 7.5, with 2 mM EDTA), with addition of 10 µL PAPs (10 mM in TRIS-buffer) after 5, 60 and 120 min of incubation. Negative control samples were prepared by omitting the tested monomer or the cofactor (UDPGA and PAPs) in order to exclude false-positive results. A positive control was included by incubating 4-NP (10 µL of 10 mM in TRIS-buffer) and monitoring the formation of 4-NP glucuronide and 4-NP sulphate. Reactions were stopped as described above for the phase I incubations.

All samples were centrifuged for 5 min at 8000 rpm (5900 g). The

Table 1
Percentage organic mobile phase (%B) used for the LC-QTOF-MS/MS analysis of the samples of the different in vitro metabolism experiments.

Time (min)	BisGMA / BisPMA	UDMA	TCD-DI-HEA
0	15	15	5
1	15	15	5
15	95	85	85
15.1	95	95	95
18	95	95	95
18.1	15	15	5
24	15	15	5

supernatant was transferred to a clean glass tube, evaporated under nitrogen at 38 °C, and reconstituted in 200 µL of a 10% (v/v) ACN in ultrapure water solution for LC-QTOF-MS analysis.

2.3. LC-QTOF-MS analytical method

Extracts were analysed using an Agilent 1290 Infinity UPLC hyphenated to an Agilent 6530 QTOF (Agilent, Santa Clara, USA). Chromatographic separation was performed on an Agilent Poroshell EC-C18 column (100 x 3.0 mm; 2.7 µm particle size, Agilent, Santa Clara, USA) using a mobile phase composed of ultra-pure water with 1 mM ammonium fluoride (A) and methanol with 1 mM ammonium fluoride (B) with a flow of 0.4 mL/min. The injection volume was 5 µL. All samples were analysed in positive and negative ionization mode. The eluent was directed to the waste during the first minute of each run to protect the ion source from extensive contamination. For the analysis different gradients were used for the investigated monomers in order to have a maximal separation of possible metabolites. An overview of the gradients can be found in Table 1. The column temperature was kept constant at 40 °C.

The QTOF-MS instrument was operated in the 2 GHz (extended dynamic range) mode, providing a Full Width at Half Maximum (FWHM) resolution of approximately 5100 at *m/z* 118.0862 and 10,000 at *m/z* 922.0098. The ions *m/z* 121.0508 and 922.0097 for positive mode and *m/z* 119.0363 and 940.0009 for negative mode were selected for constant recalibration throughout the chromatographic run to ensure high mass accuracy. The eluting compounds were ionized using Agilent Jet-Stream electrospray ionization in both positive and negative ionization mode. Drying gas temperature and flow were at 325 °C and 8 L/min, respectively. The sheath gas temperature was 325 °C at a flow of 11 L/min. Nebulizer pressure was set at 40 psig. Capillary, nozzle and fragmentor voltages were at 3500 V, 0 V and 125 V, respectively. The acquisition parameters were set for a *m/z* range from 80 to 1000 at a scan rate of 5 scans/s and 6.67 scans/s for MS and MS/MS spectra, respectively. Collision energies were applied at 10 and 30 V. Signals were detected using a data-dependent acquisition method. An active exclusion of 0.15 min was applied to prevent repetitive acquisition of MS/MS spectra for the same ion. All data were stored in centroid mode and exported for analysis.

2.4. Workflows and data analysis

This study employed a suspect screening workflow for processing the acquired *in vitro* data based on an in-house developed workflow, which has been published previously. (Mortele et al., 2018; Negreira et al., 2015, 2016) First, a list of possible biotransformation products was generated using the Meteor Nexus (v2.1, Lhasa Limited, Leeds, UK) software. For Phase I metabolism, all redox and non-redox biotransformations were selected. For Phase II metabolism, *O*- and *N*-glucuronidation, *O*- and *N*-sulfation, acetylation and conjugation with amino acids were selected. The metabolite prediction was processed with human CYP enzymes, the maximum depth set on 3 and the maximum number of biotransformation products set at 1000. The generated list of possible biotransformation products with the molecular formula, exact mass, structure and related enzyme for the corresponding metabolism was stored as a csv-database. Furthermore, the list of compounds in the database was augmented with structural information of possible metabolites predicted by hand but not by Meteor Nexus.

Identification of the biotransformation products was based on the accurate mass and isotopic profile obtained in the MS mode and on the fragmentation pattern of product ions and their accurate mass, with the following criteria: (a) a maximal mass variation of ± 15 ppm between the measured and theoretical parent ions; (b) a maximal mass variation of ± 25 ppm for product ions; (c) the measured isotope pattern matched with the predicted ones with an isotope abundance score of at least 70; (d) the identified biotransformation products were not present in any of the negative control samples; and (e) the detected biotransformation products were present in at least two out of three replicates.

3. Results and discussion

3.1. Experimental quality controls

As described in our previous study, phenacetin and 4-NP were used as positive control compounds for Phase I and Phase II respectively, to ensure the performance of the experimental setup. (Mortele et al., 2018) MS and MS/MS spectra of the identified biotransformation products were found as expected and are shown in the supporting information (Figures SI-2 to SI-6).

3.2. Detection of parent monomers

BisGMA was detected in positive ionization mode ($[M + NH_4]^+$: *m/z* 530.2766; $[M + Na]^+$: *m/z* 535.2328). Figure SI-7 shows the MS/MS spectrum and fragmentation pattern of BisGMA. Loss of water from the protonated molecule led to the formation of a product ion at *m/z* 495.2395. The neutral loss of methacrylic acid from BisGMA leads to the product ion at *m/z* 427.2046. Further loss of the 1-phenoxypropan-2-ol moiety led to product ion at *m/z* 277.1391. Product ions *m/z* 143.0704 and *m/z* 69.0333 are related to the methacrylic acid moiety of the monomer.

BisPMA was detected in positive ionization mode ($[M + NH_4]^+$: *m/z* 498.2863; $[M + Na]^+$: *m/z* 503.2417). Figure SI-8 shows the MS/MS spectrum and fragmentation pattern of BisPMA. BisPMA is structurally related to BisGMA, lacking only an oxygen atom on the 3-methacryloxypropoxy)phenyl moiety compared to BisGMA. As a result, fragment ions related to this moiety (*m/z* 261.1463, 175.1099 and 127.0740) have an *m/z* difference of 16 Da compared to the MS/MS spectrum of BisGMA. As with BisGMA, the product ion *m/z* 69.0332 is specific for the methacrylic group.

TCD-DI-HEA was detected in positive ionization mode ($[M+H]^+$: *m/z* 479.2381; $[M + NH_4]^+$: *m/z* 496.2658; $[M + Na]^+$: *m/z* 501.2207). Due to its structure three isomers could be identified for TCD-DI-HEA at a retention time of 14.31, 14.90 and 15.04 min. Figure SI-9 shows the MS/MS spectrum and fragmentation pattern of TCD-DI-HEA. Loss of an acrylic acid moiety from TCD-DI-HEA led to the formation of the product ion with *m/z* 407.2142. Further loss of an ethoxy moiety led to the product ion at *m/z* 363.1866. Subsequent loss of $C_3H_4O_2$ led to the formation of the product ion at *m/z* 291.1677. The product ions at *m/z* 99.0427 and 55.0178 are related to the acrylic acid functional group of the monomer. The difference of 14 Da of *m/z* 55.0178 to the other monomers can be explained by the absence of a methyl entity when comparing with the methacrylic acid moiety on the other monomers.

UDMA was detected in positive ionization mode ($[M+H]^+$: *m/z* 471.2718; $[M + NH_4]^+$: *m/z* 488.2979; $[M + Na]^+$: *m/z* 493.2541). Figure SI-10 shows the MS/MS spectrum and fragmentation pattern of UDMA. The loss of 86.0355 Da from the protonated molecule corresponds to the loss of the methacrylic acid moiety. Further loss of an

Table 2
Overview of all parent compounds and transformation products identified in this study. For each compound the name, molecular formula, retention time (in minutes), mass difference (expressed as ppm), measured and target mass, polarity of detection, adducts, MS/MS product ions (*m/z*) and level of confirmation according to Schymanski et al are given.

Name	Formula	RT (min)	Δ mass (ppm)	Measured Mass	Target Mass	Polarity	Adducts	MS/MS product ions	Level confirmation
BisGMA-A	C29 H36 O8	14.94	4.02	512.2431	512.2410	+	+H, +NH4, +Na	495.2309 ; 427.2046 ; 277.1391 ; 259.1285 ; 209.1136 ; 173.0929 ; 143.0681 ; 69.0324	L1
BisGMA-B	C29 H36 O8	15.22	5.64	512.2439	512.2410	+	+H, +NH4, +Na	495.2435 ; 277.1464 ; 259.1353 ; 173.0975 ; 143.0711 ; 135.0421 ; 69.0340	L1
BisGMA-M1-A	C25 H32 O7	13.58	1.17	444.2153	444.2148	+	+NH4, +Na	427.2100 ; 277.1419 ; 209.1158 ; 173.0951 ; 143.0694 ; 69.0335	L2a
BisGMA-M1-B	C25 H32 O7	14.31	−0.24	444.2147	444.2148	+	+NH4, +Na	/	L2a
BisGMA-M2-A	C21 H28 O6	11.47	0.71	376.1889	376.1886	+ / -	+NH4, +Na -H	359.1885 ; 209.1189 ; 191.1072 ; 135.0807 ; 107.0493	L3
BisGMA-M2-B	C21 H28 O6	12.56	4.83	376.1904	376.1886	+ / -	+NH4, +Na -H	209.1159 ; 191.1063 ; 173.0932 ; 161.0960 ; 149.0593 ; 131.0471 ; 119.0486	L3
BisGMA-M3	C21 H28 O7	9.34	5.36	392.1856	392.1835	+ / -	+NH4, +Na -H	225.1092 ; 207.0983 ; 189.0900 ; 177.0878 ; 165.0506 ; 135.0414	L3
BisGMA-M4	C21 H26 O7	9.83	3.16	390.1691	390.1679	–	-H	301.1418 ; 227.1069 ; 212.0760	L3
UDMA	C23 H38 N2 O8	14.65	−3.35	470.2613	470.2628	+	+H, +NH4, +Na	385.2306 ; 241.2046 ; 255.1692 ; 113.0600 ; 69.0342	L1
UDMA-M1	C19 H34 N2 O7	12.57	2.67	402.2377	402.2366	+	+H, +Na	341.2093 ; 273.1802 ; 255.1693 ; 168.1385 ; 113.0601 ; 69.0343	L3
UDMA-M2	C15 H30 N2 O6	9.85	3.96	334.2117	334.2104	+	+H, +Na	317.2075 ; 273.1815 ; 255.1710 ; 229.1917 ; 211.1446 ; 168.1387	L3
UDMA-M3	C15 H28 N2 O6	9.08	2.19	332.1955	332.1947	+	+H, +Na	/	L4
BisPMA	C29 H36 O6	16.857	−3.32	480.2496	480.2512	+	+NH4, +Na	261.1463 ; 175.1099 ; 127.0740 ; 69.0332	L1
BisPMA-M1	C21 H28 O4	13.72	6.71	344.2011	344.1988	+	+H, +NH4, +Na	193.1231 ; 135.0808 ; 107.0499	L3
BisPMA-M2	C21 H26 O5	11.62	5.84	358.1801	358.1780	+ / -	+Na, -H	285.1491 ; 227.1067 ; 211.0754 ; 133.0644	L3
BisPMA-M3	C21 H24 O6	8.87	3.26	372.1585	372.1573	–	-H	353.2088 ; 299.1276 ; 227.1026 ; 212.0827	L3
BisPMA-M4	C18 H22 O3	12.86	5.77	286.1585	286.1569	–	-H	267.1971 ; 227.1077 ; 211.0767 ; 133.0641 ; 93.0362	L3
BisPMA-M5	C18 H20 O4	10.48	1.84	300.1367	300.1362	–	-H	227.1086 ; 212.0844 ; 133.0670 ; 93.0351	L3
BisPMA-M6	C15 H16 O2	10.48	0.20	228.1151	228.1150	–	-H	/	L1
BisPMA-M7	C18 H22 O4	11.98	1.72	302.1524	302.1518	–	-H	/	L4
BisPMA-M8	C18 H20 O5	9.55	1.95	316.1317	316.1311	–	-H	/	L4
BisPMA-M9	C27 H36 O10	11.56	6.61	520.2343	520.2308	+ / -	+NH4, +Na, -H	501.2066 ; 459.1966 ; 285.1480 ; 227.1060 ; 211.0748 ; 113.0239 ; 85.0293 ; 75.0095	L3
BisPMA-M10	C21 H28 O7 S	11.96	−2.84	424.1544	424.1556	–	-H	285.1481 ; 227.1072 ; 211.0738 ; 136.9911 ; 96.9592	L3
BisPMA-M11	C18 H22 O6 S	10.62	0.74	366.1140	366.1137	–	-H	329.2290 ; 285.1451 ; 227.1035 ; 211.0739 ; 79.9568	L3
BisPMA-M12	C18 H20 O7 S	7.82	0.23	380.0931	380.0930	–	-H	/	L4
TCD-DI-HEA-A	C24 H34 N2 O8	14.31	3.23	478.2331	478.2315	+	+H, +NH4, +Na	407.2119 ; 363.1850 ; 291.1659 ; 117.0524 ; 99.0425 ; 55.0174	L1
TCD-DI-HEA-B	C24 H34 N2 O8	14.90	−5.26	478.2290	478.2315	+	+H, +NH4, +Na	407.2142 ; 363.1866 ; 291.1677 ; 117.0532 ; 99.0427 ; 55.0178	L1
TCD-DI-HEA-C	C24 H34 N2 O8	15.04	−9.20	478.2271	478.2315	+	+H, +NH4, +Na	407.2156 ; 363.1904 ; 353.2075 ; 309.1808 ; 291.1700 ; 204.1383 ; 117.0542 ; 99.0442 ; 55.0185	L1
TCD-DI-HEA-M1-A	C21 H32 N2 O7	13.08	−3.07	424.2196	424.2210	+	+H, +Na	407.2156 ; 353.2075 ; 309.1808 ; 291.1700 ; 204.1383 ; 117.0542 ; 99.0442 ; 55.0185	L3
TCD-DI-HEA-M1-B	C21 H32 N2 O7	13.85	5.96	424.2235	424.2210	+	+H, +Na	407.2197 ; 353.2102 ; 309.1832 ; 291.1731 ; 204.1394 ; 117.0550 ; 99.0447 ; 55.0189	L3
TCD-DI-HEA-M1-C	C21 H32 N2 O7	14.01	0.93	424.2213	424.2210	+	+H, +Na	407.2160 ; 353.2055 ; 309.1793 ; 291.1689 ; 247.1427 ; 204.1369 ; 117.0537 ; 99.0433 ; 55.0183	L3
TCD-DI-HEA-M2-A	C18 H30 N2 O6	11.54	2.53	370.2113	370.2104	+	+H, +Na	353.2047 ; 309.1794 ; 291.1684 ; 204.1372 ; 161.1312	L3
TCD-DI-HEA-M2-B	C18 H30 N2 O6	12.55	−0.83	370.2101	370.2104	+	+H, +Na	353.2052 ; 309.1789 ; 291.1692 ; 204.1370 ; 161.1308	L3
TCD-DI-HEA-M2-C	C18 H30 N2 O6	12.76	1.31	370.2109	370.2104	+	+H, +Na	353.2054 ; 309.1791 ; 291.1690 ; 247.1426 ; 204.1371 ; 161.1314	L3
TCD-DI-HEA-M3-A	C18 H28 N2 O6	8.36	2.87	368.1958	368.1947	+	+H	307.1654 ; 264.1588 ; 202.1219 ; 159.1164 ; 118.0491 ; 81.0689	L3
TCD-DI-HEA-M3-B	C18 H28 N2 O6	8.79	0.22	368.1948	368.1947	+	+H	307.1643 ; 264.1584 ; 202.1218 ; 159.1160 ; 81.0698	L3

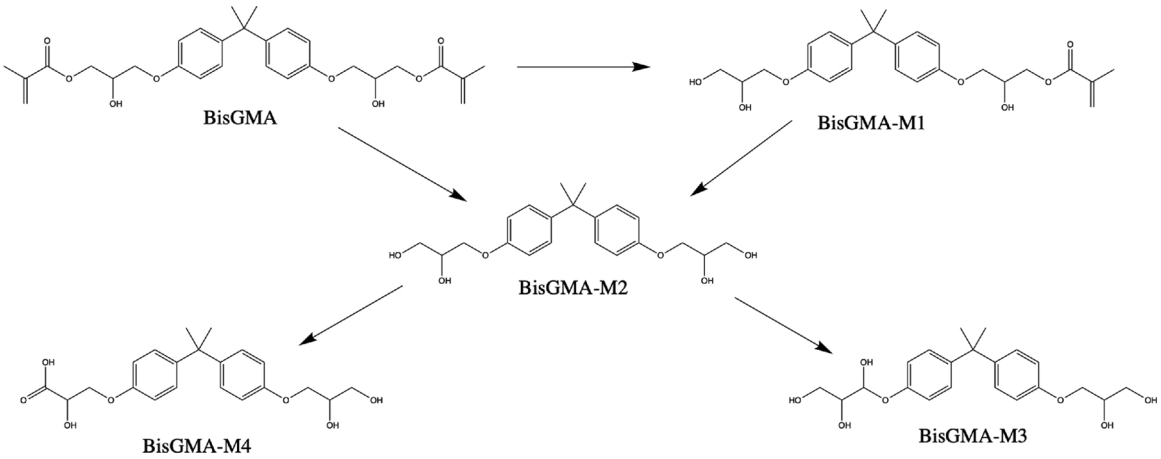

Fig. 1. Elucidated metabolic pathway of the in vitro biotransformation of BisGMA.

ethoxy group led to the product ion at *m/z* 341.2046. A subsequent neutral loss of $C_4H_6O_2$, originating from the remaining methacrylic acid moiety, resulted in the product ion at *m/z* 255.1692. The product ions at *m/z* 113.0600 and 69.0348 are related to the methacrylic acid moiety of UDMA. Both are 14 Da higher than the corresponding fragments of TCD-DI-HEA due to the presence of the extra methyl when compared to the acrylic acid of TCD-DI-HEA.

3.3. Phase I biotransformation products

An overview of all identified *in vitro* biotransformation products can be found in Table 2. Acquired MS/MS spectra can be found in the Supporting Information (Figures SI-11 to SI-27).

3.3.1. BisGMA

Figure presents an overview of the elucidated potential metabolic pathway. The parent molecule could only be detected in the negative control samples of the phase I incubation where no HLM was added. In the same sample, a monomethacrylate of BisGMA (BisGMA-M1) could also be detected. Earlier work showed this is an impurity related to the production of BisGMA (Vervliet et al., 2018a).

When incubated in HLM BisGMA was rapidly metabolized to the tetrahydroxy metabolite bisphenol A bis(2,3-dihydroxypropyl)ether (BisGMA-M2), a biotransformation product previously described by Kostoryz et al (Kostoryz et al., 2003). Two chromatographically separated peaks could be observed for this compound suggesting the presence of two different structural isomers (BisGMA-M2A & BisGMA-M2B). However, we could not further elucidate the molecular structures based on the MS/MS spectra.

BisGMA-M2 was also identified in the negative control samples where NAPDH was absent, showing that the biotransformation pathway of BisGMA-M2 is NADPH-independent. In addition, the degradation of bisphenol A diglycidyl ether (BADGE) in an aqueous environment leads to the formation of this biotransformation product (Lane et al., 2015). Therefore, this biotransformation product and all biotransformation products originating from BisGMA-M2 are no unique biomarker for human exposure to BisGMA.

Further hydroxylation of BisGMA-M2 led to the formation of BisGMA-M3. The product ion at *m/z* 225.1092 differs 16 Da from the 209.1189 product ion of BisGMA-M2A confirming the extra oxygen on this part of the molecule. Loss of water leads to the formation of the product ion at *m/z* 207.0983. Ramanathan et al and Holcapek et al have demonstrated that the loss of water from analytes in LC−MS/MS is not favoured when the hydroxylation occurred on phenyl groups (Holcapek et al., 2010; Ramanathan et al., 2000). Presence of the product ion *m/z* 207.0983 thus suggests a hydroxylation either on one of the central methyl groups or the dihydroxypropyl moiety. The product ions with *m/z* 165.0506 and 135.0414 had a predicted formula of respectively $C_9H_9O_3^+$ and $C_8H_7O_2^+$ resulting in the postulated structures and thus suggesting the hydroxylation to occur on the dihydroxypropyl moiety.

The carboxylic acid biotransformation product (BisGMA-M4), originating from further oxidation of BisGMA-M2 eluted after 9.83 min and was detected as the deprotonated ion in ESI-. Loss of the 2-hydroxypropanoic acid moiety led to the product ion with *m/z* 301.1418. Further loss of the dihydroxypropyl moiety led to the product ion at *m/z* 227.1069 (Fig. 1)

3.3.2. BisPMA

Fig. 2 presents an overview of the elucidated potential metabolic pathway. Unlike with BisGMA, no monomethacrylate could be detected in the negative control samples, indicating this was not present as an impurity from production.

Incubation of BisPMA with HLM led to a NADPH-independent formation of the dihydroxy biotransformation product by the hydrolysis of the ester functions linking the methacrylate groups (BisPMA-M1). The characteristic ions for the related to the methacrylic acid moiety (*m/z* 69.0332, 127.0740 and 261.1463) were not present in the spectra of BisPMA-M1, indicating the absence of this functional group. For the product ion at *m/z* 193.1231 a formula of $C_{12}H_{17}O_2^+$ was predicted, confirming the absence of the methacrylic acid moiety and allowing a confirmation of level 3 according to Schymanski et al (Schymanski et al., 2014).

Further hydroxylation of BisPMA-M1 led to the monocarboxylic acid BisPMA-M2 and the dicarboxylic acid BisPMA-M3. BisPMA-M2 and BisPMA-M3 shared the product ion 227.1067, confirming their BPA core. Loss of a propanoic acid moiety led to product ion *m/z* 285.1491 in BisPMA-M2 and 299.1276 in BisPMA-M3. The difference of 14 Da is explained by the different functional group on the remaining propoxy moiety.

An O-dealkylation of BisPMA-M1 led to the biotransformation product BisPMA-M4. A second O-dealkylation formed the biotransformation product BisPMA-M6 (BPA). The product ions *m/z* 227.1077 and 211.0767 confirmed the presence of the BPA core. The product ion *m/z* 267.1971 originates from the loss of water from the precursor ion. For BisPMA-M6 no MS/MS spectra could be acquired due to the lower intensity of the signal. It could still be confirmed at level 1 according to Schymanski et al due to the matching retention time and isotopic pattern with the analytical reference standard.

BisPMA-M4 was further oxidated to form the carboxylic acid BisPMA-M5. The absence of fragment ion *m/z* 267.1971 confirms the modification of the hydroxyl moiety resulting in the absence of loss of water. The other product ions confirmed the BPA-core of BisPMA-M5.

BisPMA-M7 was formed through the hydroxylation of BisPMA-M4. Further oxidation of BisPMA-M7 led to the carboxylic acid BisPMA-M8.

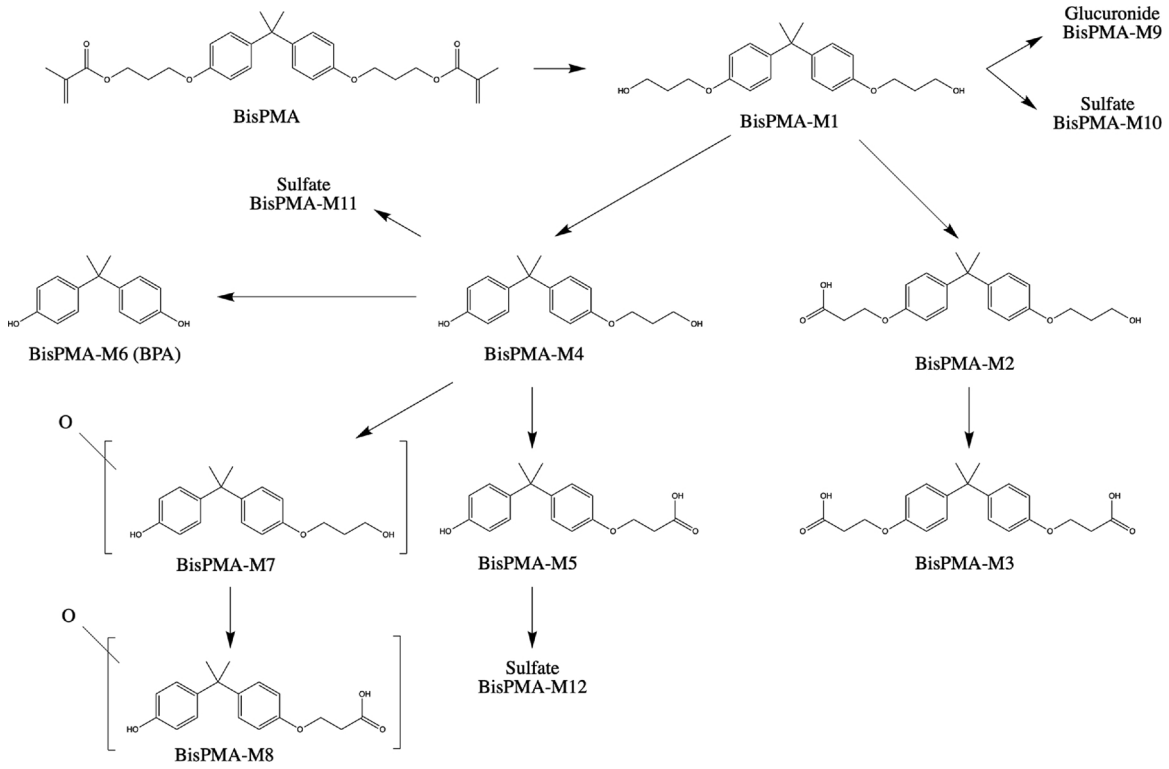

Fig. 2. Elucidated metabolic pathway of the in vitro biotransformation of BisPMA.

However, for both biotransformation products no MS/MS spectra could be acquired to raise their level of confirmation.

3.3.3. UDMA

Fig. 3 presents an overview of the elucidated potential metabolic pathway. UDMA and its monomethacrylate transformation product UDMA-M1 were only detected in the negative control samples where no HLMs were added. Incubation of UDMA with HLMs led to the rapid formation of the biotransformation product UDMA-M2. UDMA-M2 is the results of a ester hydrolysis reaction where both methacrylate moieties are removed from UDMA. The absence of the product ions related to the methacrylic acid moiety present in the spectra of UDMA with *m/z* 69.0342, 113.0600 and 131.0701 aided in the confirmation of this biotransformation product. The product ion with *m/z* 317.2075 was formed through the loss of water from the parent ion. Further loss of C_2H_4O led to the product ion at *m/z* 273.1815.

Further oxidation of UDMA-M2 formed the aldehyde UDMA-M3, which eluted after 9.08 min. The isotopic pattern match and the presence of different adducts allowed a confirmation of level 4 according to Schymanski et al, as no MS/MS spectra could be acquired (Schymanski et al., 2014).

Although (non-specific) esterases quickly hydrolysed the ester bonds of the methacrylic acid moieties, the carbamates present in UDMA did not appear to be subjected to biotransformation reactions as no related biotransformation products could be identified using our suspect screening approaches.

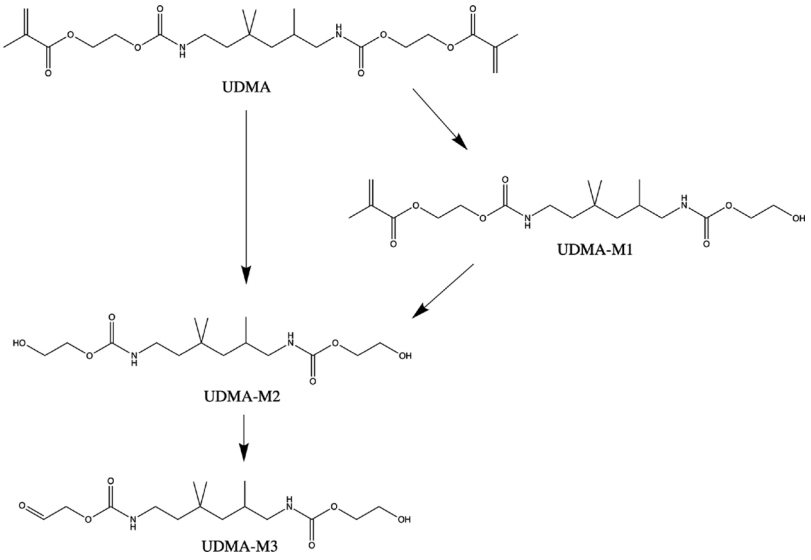

Fig. 3. Elucidated metabolic pathway of the in vitro biotransformation of UDMA.

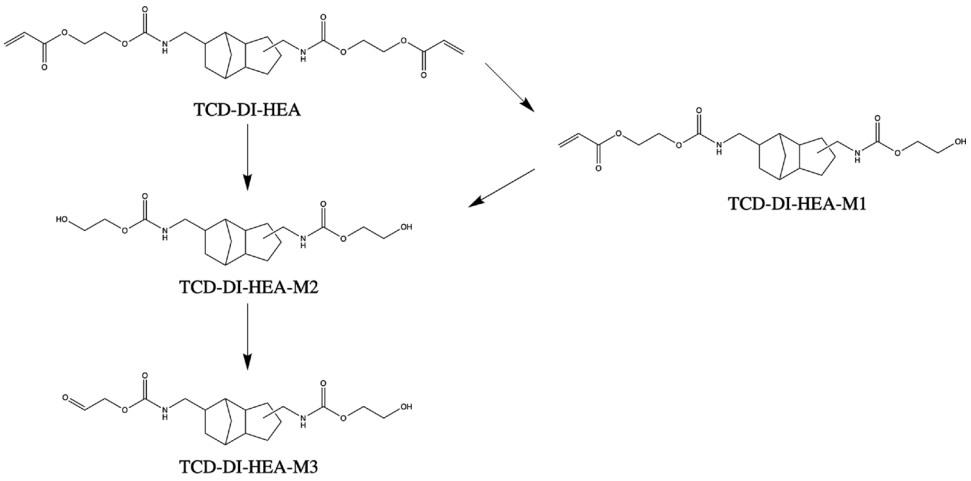

Fig. 4. Elucidated metabolic pathway of the in vitro biotransformation of TCD-DI-HEA.

3.3.4. TCD-DI-HEA

Fig. 4 presents an overview of the elucidated potential metabolic pathway. In the negative control sample where no HLM was present, three isomers of the monoacrylate transformation product TCD-DI-HEA-M1 eluted after 13.08, 13.85 and 14.01 min. For all isomers, the product ions at *m/z* 55.0189, 99.0447 and 117.0550 confirmed the presence of the remaining acrylate moiety. The product ions 407.2197 and 291.1731 were also observed with TCD-DI-HEA and confirmed, next to the other product ions, the transformation product. Incubating TCD-DI-HEA with HLMs resulted in a complete NAPDH-independent formation of the biotransformation product TCD-DI-HEA-M2. This could be confirmed by the absence of the product ions with *m/z* 55.0189, 99.0447 and 117.0550 and the presence of product ions 161.1308, 204.1370 and 309.1789 related to the core structure of TCD-DI-HEA. The loss of water from the precursor ion and the product ion with *m/z* 309.1789 led respectively to the product ions 353.2052 and 291.1692. Further oxidation of one of the hydroxyls led to the aldehyde biotransformation product TCD-DI-HEA-M3 which could be confirmed by the product ions 264.1584 and 307.1643. No further oxidative biotransformation products (e.g. carboxylic acid) were identified.

3.4. Phase II biotransformation products

The main drug metabolizing enzymes for Phase II biotransformation reactions include UDP-glucuronosyltransferases (UGTs), sulfotransferases (SULTs) and N-acetyltransferases (NATs) (Jancova et al., 2010). UGTs and NATs were present in the HLMs and SULTs were present in the HLCYTs used in this study. The formation of p-nitrophenyl-glucuronide and p-nitrophenyl-sulphate proved the capability of our experimental assay to form these conjugates, as was the case in previous experiments using this experimental setup (Mortele et al., 2018; Vervliet et al., 2018b).

During Phase II reactions, BisPMA-M1 was conjugated with glucuronic acid or sulphate to form respectively BisPMA-M9 and BisPMA-M10. The common fragments at *m/z* 285.1480, 227.1060 and 211.0748 confirmed their shared origin. BisPMA-M9 could be further confirmed with product ion *m/z* 401.1965 and 501.2066. BisPMA-M10 could be further confirmed with the product ions *m/z* 136.9911 and 96.9592 which are related to the sulphate moiety.

BisPMA-M4 was conjugated with sulphate and formed BisPMA-M11. Loss of the sulphate moiety led to the product ion at *m/z* 285.1451, which confirms the origin of BisPMA-M4. The product ions 227.1035 and 211.0739 are also shared with BisPMA-M4. The product ion at 79.9568 originates from the sulphate moiety and confirms its presence in BisPMA-M11.

BisPMA-M5 was conjugated with sulphate during Phase II reactions to form BisPMA-M12. However, no MS/MS spectra could be acquired for BisPMA-M12 to raise the level of confirmation.

However, besides for BisPMA no Phase II conjugation biotransformation products could be detected for any of the tested resin monomers. Meteor Nexus only predicted conjugation reactions with glutathione for the dental resin monomers after Phase I reactions. Although glutathione S-transferase (GST) was present in the cytosolic fractions, these conjugates could not be formed in our assay as the necessary cofactor was not present. Secondly, possible acetyl conjugates could not be formed as the necessary cofactor (acetyl CoA) was not added during the experiment and thus not available for the NATs present in the used subcellular fractions.

As enzymatic cleavage is an often-used technique for sample preparation in both forensic and environmental urine analysis (Bastiaensen et al., 2018; Geens et al., 2009; Maurer, 2007; Silva et al., 2004; Xue et al., 2015), the Phase I biotransformation products identified in this study can be a possible target for biomonitoring studies after dental restorations.

3.5. Time trends of the Phase I biotransformation products

Fig. 5 shows the time trends of the phase I biotransformation products. For each biotransformation product, the relative area was calculated by dividing the area by the area of the internal standard theophylline and the average per group was plotted. The control group consists of samples where HLM and substrate were added but no NADPH was added. Parent compound and the mono(meth)acrylate impurity were not plotted for all tested compounds as they were not detected in any of these three groups.

For all substrates, the secondary biotransformation products (BisGMA-M3, BisPMA-M2 to BisPMA-M7, TCD-DI-HEA-M3 and UDMA-M3) show an increase over time confirming them as possible targets for biomonitoring studies. Table 3 summarises the formation of the different biotransformation products and their possible application as biomarker.

3.6. Toxicity of biotransformation products

Although liver metabolism serves as a detoxification mechanism, biotransformation products can still interfere with hormones in the tissues where they are generated (Zoeller et al., 2012). The effects of BPA, identified as a biotransformation product of BisPMA, have been widely studied and reviewed, with its potential estrogenic, anti-androgenic and thyroid activity being evidenced (Howdeshell et al., 1999;

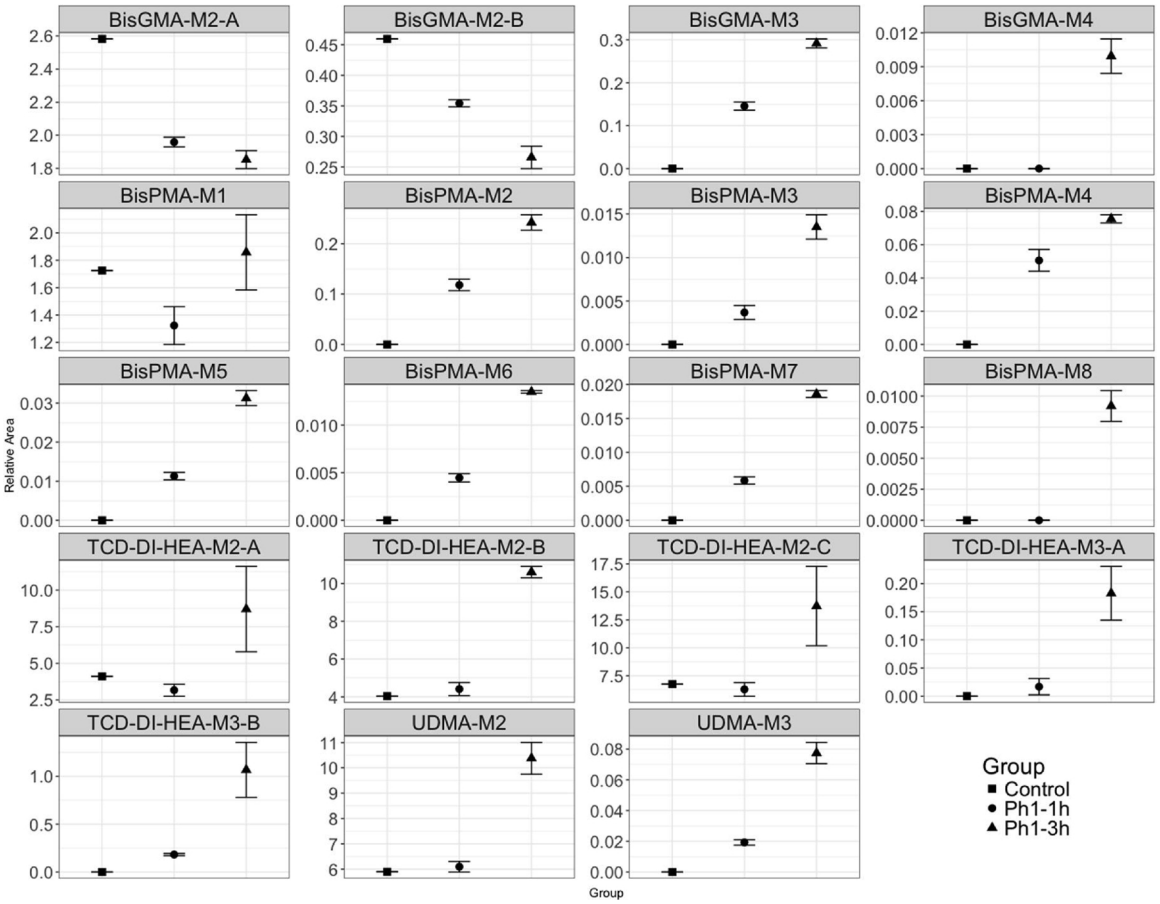

Fig. 5. Time Trends Phase I biotransformation products. For each biotransformation product the average relative area is calculated by dividing the area of the biotransformation product by the area of the area of the internal standard theophylline. Per group results are averaged and standard deviations are shown.

Table 3
Overview of the different biotransformation products. For each biotransformation product the possibility to be used as a unique biomarker is marked, as well as the different biotransformation reactions resulting in the specific product.

			Phase I biotransformation reactions				Phase II conjugations	
	Biotransformation product	Possible biomarker	(Meth)acrylic acid ester hydrolysis	Hydroxylation	O-dealkylation	Oxidation	Glucuronic acid	Sulphate
BisGMA	M1		X					
	M2		X					
	M3		X	X				
	M4		X	X				
BisPMA	M1		X					
	M2	X	X			X		
	M3	X	X			X		
	M4	X	X		X			
	M5	X	X		X	X		
	M6		X		X			
	M7		X	X	X			
	M8		X	X	X	X		
	M9		X				X	
	M10		X					X
	M11		X		X			X
	M12		X		X	X		X
TCD-DI-HEA	M1		X					
	M2		X					
	M3	X	X			X		
UDMA	M1		X					
	M2		X					
	M3	X	X			X		

Kuiper et al., 1998; Vandenberg et al., 2009). Although BPA was only identified in BisPMA, several studies report higher salivary and urinary concentrations of BPA after routine use of dental materials (Kloukos et al., 2013). However, previous studies may have overestimated BPA exposure from dental treatments either due to analytical interference due to co-elution of compounds or by using ELISA which may overestimate BPA concentrations in biological samples (Chapin et al., 2008). It thus remains unclear how much BPA is released during and after dental treatment.

For BisGMA-M2 (also known as BADGE.2H_2O), limited data exists on adverse effects. BADGE.2H_2O increased the expression of Nur77 mRNA and protein as well as the promotor activity and transactivation of Nur77 in mouse testicular Leydig cells, suggesting a disruption of testicular steroidogenesis (Ahn et al., 2008). Estrogenic and androgenic activities have been tested for BisGMA and BisGMA-M2. Whereas BisGMA exerted a weak anti-estrogenic activity, the hydrolysed product BisGMA-M2 had no (anti)estrogenic or (anti)androgenic activity (Fic et al., 2014).

Other biotransformation products identified in our study have not been studied and their effects on the human body remain unknown. Due to its structural resemblance to BisGMA, BisPMA and its metabolites might exert equal effects as BisGMA in the human body and needs to be investigated. In addition, a recent study by Karrer et al suggests glucuronide conjugates may not be devoid of pharmacological activity, although previous reviews described the Phase II conjugation of BPA as detoxification reactions (Goodman et al., 2009; Karrer et al., 2018).

4. Conclusions

Incubating dental monomers with HLMs leads to a complete hydrolysis of the ester groups linking the (meth)acrylates to the core of the monomer, without the need for NADPH.

After hydrolysis, oxidative pathways transformed a hydroxyl group to an aldehyde for UDMA and TCD-DI-HEA. For BisGMA, the demethacrylated biotransformation product was further metabolized to a hydroxylated and a carboxylic acid biotransformation product. Although it structurally resembles to BisGMA, BisPMA was the most extensively metabolized dental monomer with 12 identified biotransformation products. The secondary products were formed through oxidative and hydroxylation pathways, followed by conjugation with glucuronic acid and sulphate. For the other monomers no Phase II conjugates could be identified. The monomers in this study lacking the BPA-core (UDMA and TCD-DI-HEA) had carbamate functions which appeared to be resistant to biotransformation reactions as no corresponding biotransformation products were observed. Except for BisGMA, possible biomarkers for detection in biomonitoring studies have been identified for the tested monomers.

Conflicts of interest

The authors declare they have no conflict of interest.

Acknowledgements

This study acknowledges the provision of funding through a Research Foundation Flanders (FWO) project (G089016N). The authors would like to acknowledge the manufacturers Esstech Inc, Kulzer and 3 M ESPE for providing the standards used in this study.

Appendix A. Supplementary data

Supplementary material related to this article can be found, in the online version, at doi:https://doi.org/10.1016/j.tox.2019.03.007.

References

Ahn, S.-W., Nedumaran, B., Xie, Y., Kim, D.-K., Kim, Y.D., Choi, H.-S., 2008. Bisphenol a bis(2,3-dihydroxypropyl) ether (BADGE.2H2O) induces orphan nuclear receptor Nur77 gene expression and increases steroidogenesis in mouse testicular leydig cells. Mol. Cells 26, 74–80.
Al-Hiyasat, A.S., Darmani, H., 2006. In vivo effects of BISGMA—a component of dental composite—on male mouse reproduction and fertility. J. Biomed. Mater. Res. A. 78A, 66–72.
Ballesteros-Gomez, A., Erratico, C.A., Van den Eede, N., Ionas, A.C., Leonards, P.E.G., Covaci, A., 2015. In vitro metabolism of 2-ethylhexyldiphenyl phosphate (EHDPHP) by human liver microsomes. Toxicol. Lett. 232, 203–212.
Bastiaensen, M., Xu, F., Been, F., Van den Eede, N., Covaci, A., 2018. Simultaneous determination of 14 urinary biomarkers of exposure to organophosphate flame retardants and plasticizers by LC-MS/MS. Anal. Bioanal. Chem.
Bonefeld-Jørgensen, E.C., Long, M., Hofmeister, M.V., Vinggaard, A.M., 2007. Endocrine-disrupting potential of bisphenol a, bisphenol a dimethacrylate, 4-n-Nonylphenol, and 4-n-Octylphenol in vitro : new data and a brief review. Environ. Health Perspect. 115, 69–76.
Brandon, E.F.A., Raap, C.D., Meijerman, I., Beijnen, J.H., Schellens, J.H.M., 2003. An update on in vitro test methods in human hepatic drug biotransformation research: pros and cons. Toxicol. Appl. Pharmacol. 189, 233–246.
Burmaster, S., Smith, R., Eick, D., Kostoryz, E.L., Yourtee, D., 2002. In-vitro stability, metabolism, and transport of dental monomers made from bisphenol A and bisphenol F. Macromol. Biosci. 2, 365–379.
Chapin, R.E., Adams, J., Boekelheide, K., Gray Jr., L.E., Hayward, S.W., Lees, P.S., McIntyre, B.S., Portier, K.M., Schnorr, T.M., Selevan, S.G., Vandenbergh, J.G., Woskie, S.R., 2008. NTP-CERHR expert panel report on the reproductive and developmental toxicity of bisphenol A. Birth Defects Res. B Dev. Reprod. Toxicol. 83, 157–395.
Durner, J., Kreppel, H., Zaspel, J., Schweikl, H., Hickel, R., Reichl, F.X., 2009. The toxicokinetics and distribution of 2-hydroxyethyl methacrylate in mice. Biomaterials 30, 2066–2071.
Dursun, E., Fron-Chabouis, H., Attal, J.P., Raskin, A., 2016. Bisphenol a release: survey of the composition of dental composite resins. Open Dent. J. 10, 446–453.
Erratico, C., Zheng, X.B., van den Eede, N., Tomy, G., Covaci, A., 2016. Stereoselective Metabolism of alpha-, beta-, and gamma-Hexabromocyclododecanes (HBCDs) by Human Liver Microsomes and CYP3A4. Environ. Sci. Technol. 50, 8263–8273.
Fic, A., Zegura, B., Gramec, D., Masic, L.P., 2014. Estrogenic and androgenic activities of TBBA and TBMEPH, metabolites of novel brominated flame retardants, and selected bisphenols, using the XenoScreen XL YES/YAS assay. Chemosphere 112, 362–369.
Fisher, M.B., Campanale, K., Ackermann, B.L., Vandenbranden, M., Wrighton, S.A., 2000. In vitro glucuronidation using human liver microsomes and the pore-forming peptide alamethicin. Drug Metab. Dispos. 28, 560–566.
Forss, H., Widström, E., 2001. From amalgam to composite: selection of restorative materials and restoration longevity in Finland. Acta Odontol. Scand. 59, 57–62.
Geens, T., Neels, H., Covaci, A., 2009. Sensitive and selective method for the determination of bisphenol-A and triclosan in serum and urine as pentafluorobenzoate-derivatives using GC-ECNI/MS. J. Chromatogr. B Anal. Technol. Biomed. Life Sci. 877, 4042–4046.
Goodman, J.E., Witorsch, R.J., McConnell, E.E., Sipes, I.G., Slayton, T.M., Yu, C.J., Franz, A.M., Rhomberg, L.R., 2009. Weight-of-Evidence evaluation of reproductive and developmental effects of low doses of bisphenol a. Crit. Rev. Toxicol. 39, 1–75.
Gupta, S.K., Saxena, P., Pant, V.A., Pant, A.B., 2012. Release and toxicity of dental resin composite. Toxicol. Int. 19, 225–234.
Hewitt, N.J., Buhring, K.U., Dasenbrock, J., Haunschild, J., Ladstetter, B., Utesch, D., 2001. Studies comparing in vivo:in vitro metabolism of three pharmaceutical compounds in rat, dog, monkey, and human using cryopreserved hepatocytes, microsomes, and collagen gel immobilized hepatocyte cultures. Drug Metab. Dispos. 29, 1042–1050.
Holcapek, M., Jirasko, R., Lisa, M., 2010. Basic rules for the interpretation of atmospheric pressure ionization mass spectra of small molecules. J. Chromatogr. A 1217, 3908–3921.
Howdeshell, K.L., Hotchkiss, A.K., Thayer, K.A., Vandenbergh, J.G., vom Saal, F.S., 1999. Exposure to bisphenol A advances puberty. Nature 401, 763–764.
Jancova, P., Anzenbacher, P., Anzenbacherova, E., 2010. Phase II drug metabolizing enzymes. Biomed. Pap. Med. Fac. Univ. Palacky Olomouc Czech. 154, 103–116.
Jia, L., Liu, X., 2007. The conduct of drug metabolism studies considered good practice (II): in vitro experiments. Curr. Drug Metab. 8, 822–829.
Joskow, R., Barr, D.B., Barr, J.R., Calafat, A.M., Needham, L.L., Rubin, C., 2006. Exposure to bisphenol A from bis-glycidyl dimethacrylate–based dental sealants. J. Am. Dent. Assoc. 137, 353–362.
Karrer, C., Roiss, T., von Goetz, N., Gramec Skledar, D., Peterlin Mašič, L., Hungerbühler, K., 2018. Physiologically based pharmacokinetic (PBPK) modeling of the bisphenols BPA, BPS, BPF, and BPAF with new experimental metabolic parameters: comparing the pharmacokinetic behavior of BPA with its substitutes. Environ. Health Perspect. 126.
Khalaf, M.E., Alomari, Q.D., Omar, R., 2014. Factors relating to usage patterns of amalgam and resin composite for posterior restorations - a prospective analysis. J. Dent. 42, 785–792.
Kingman, A., Hyman, J., Masten, S.A., Jayaram, B., Smith, C., Eichmiller, F., Arnold, M.C., Wong, P.A., Schaeffer, J.M., Solanki, S., Dunn, W.J., 2012. Bisphenol A and other compounds in human saliva and urine associated with the placement of composite restorations. J. Am. Dent. Assoc. 143, 1292–1302.
Kloukos, D., Pandis, N., Eliades, T., 2013. In vivo bisphenol-a release from dental pit and

fissure sealants: a systematic review. J. Dent. 41, 659–667.
Knights, K.M., Stresser, D.M., Miners, J.O., Crespi, C.L., 2016. In vitro drug metabolism using liver microsomes. Curr. Protoc. Pharmacol. 74 7.8.1.-7.8.24.
Kostoryz, E.L., Eick, J.D., Glaros, A.G., Burmaster, S., Yourtee, D.M., 2003. Biocompatibility of hydroxylated metabolites of BISGMA and BFDGE. J. Dent. Res. 82, 367–371.
Kuiper, G.G.J.M., Lemmen, J.G., Carlsson, B., Corton, J.C., Safe, S.H., Van Der Saag, P.T., Van Der Burg, B., Gustafsson, J.A., 1998. Interaction of estrogenic chemicals and phytoestrogens with estrogen receptor β. Endocrinology 139, 4252–4263.
Lai, F.Y., Erratico, C., Kinyua, J., Mueller, J.F., Covaci, A., van Nuijs, A.L.N., 2015. Liquid chromatography-quadrupole time-of-flight mass spectrometry for screening in vitro drug metabolites in humans: investigation on seven phenethylamine-based designer drugs. J. Pharm. Biomed. Anal. 114, 355–375.
Lane, R.F., Adams, C.D., Randtke, S.J., Carter Jr., R.E., 2015. Bisphenol diglycidyl ethers and bisphenol A and their hydrolysis in drinking water. Water Res. 72, 331–339.
Lempel, E., Czibulya, Z., Kunsági-Máté, S., Szalma, J., Sümegi, B., Böddi, K., 2014. Quantification of conversion degree and monomer elution from dental composite using HPLC and micro-raman spectroscopy. Chromatographia 77, 1137–1144.
Lynch, C., Wilson, N., 2013. Managing the phase-down of amalgam: part I. Educationaland training issues. Br. Dent. J. 215, 109–113.
Maffini, M.V., Rubin, B.S., Sonnenschein, C., Soto, A.M., 2006. Endocrine disruptors and reproductive health: the case of bisphenol-A. Mol. Cell. Endocrinol. 254-255, 179–186.
Mariotti, A., Söderholm, K.-J., Johnson, S., 1998. The in vivo effects of bisGMA on murine uterine weight, nucleic acids and collagen. Eur. J. Oral Sci. 106, 1022–1027.
Maserejian, N.N., Trachtenberg, F.L., Wheaton, O.B., Calafat, A.M., Ranganathan, G., Kim, H.Y., Hauser, R., 2016. Changes in urinary bisphenol A concentrations associated with placement of dental composite restorations in children and adolescents. J. Am. Dent. Assoc. 147, 620–630.
Maurer, H.H., 2007. Current role of liquid chromatography-mass spectrometry in clinical and forensic toxicology. Anal. Bioanal. Chem. 388, 1315–1325.
McKinney, C., Rue, T., Sathyanarayana, S., Martin, M., Seminario, A.L., DeRouen, T., 2014. Dental sealants and restiorations and urinary bisphenol A concentrations in children in the 2003-2004 National Health and Nutrition Examination Survey. J. Am. Dent. Assoc. 145, 745–750.
Mortele, O., Vervliet, P., Gys, C., Degreef, M., Cuykx, M., Maudens, K., Covaci, A., van Nuijs, A.L.N., Lai, F.Y., 2018. In vitro Phase I and Phase II metabolism of the new designer benzodiazepine cloniprazepam using liquid chromatography coupled to quadrupole time-of-flight mass spectrometry. J. Pharm. Biomed. Anal. 153, 158–167.
Negreira, N., Erratico, C., Kosjek, T., van Nuijs, A.L., Heath, E., Neels, H., Covaci, A., 2015. In vitro Phase I and Phase II metabolism of alpha-pyrrolidinovalerophenone (alpha-PVP), methylenedioxypyrovalerone (MDPV) and methedrone by human liver microsomes and human liver cytosol. Anal. Bioanal. Chem. 407, 5803–5816.
Negreira, N., Erratico, C., van Nuijs, A.L., Covaci, A., 2016. Identification of in vitro metabolites of ethylphenidate by liquid chromatography coupled to quadrupole time-of-flight mass spectrometry. J. Pharm. Biomed. Anal. 117, 474–484.
Olea, N., Pulgar, R., Perze, P., Olea-Serrano, F., Rivas, A., Novillo-Fertrell, A., Pedraza, V., Soto, A.M., Sonnenschein, C., 1996. Estrogenicity of resin-based composites and sealants used in dentistry. Environ. Health Perspect. 104, 298–305.
Pongprueksa, P., De Munck, J., Duca, R.C., Poels, K., Covaci, A., Hoet, P., Godderis, L., Van Meerbeek, B., Van Landuyt, K.L., 2015. Monomer elution in relation to degree of conversion for different types of composite. J. Dent. 43, 1448–1455.
Ramanathan, R., Su, A.-D., Alvarez, N., Blumenkrantz, N., Chowdhury, S.K., Alton, K., Patrick, J., 2000. Liquid chromatography/mass spectrometry methods for distinguishing N-Oxides from hydroxylated compounds. Anal. Chem. 72, 1352–1359.
Reichl, F.X., Durner, J., Hickel, R., Kunzelmann, K.H., Jewett, A., Wang, M.Y., Spahl, W., Kreppel, H., Moes, G.W., Kehe, K., Walther, U., Forth, W., Hume, W.R., 2001. Distribution and excretion of TEGDMA in guinea pigs and mice. J. Dent. Res. 80, 1412–1415.
Reichl, F.X., Durner, J., Kehe, K., Manhart, J., Folwaczny, M., Kleinsasser, N., Hume, W.R., Hickel, R., 2002. Toxicokinetic of HEMA in guinea pigs. J. Dent. 30, 353–358.
Reichl, F.X., Seiss, M., Kleinsasser, N., Kehe, K., Kunzelmann, K.H., Thomas, P., Spahl, W., Hickel, R., 2008. Distribution and excretion of BisGMA in guinea pigs. J. Dent. Res. 87, 378–380.
Richter, L.H.J., Flockerzi, V., Maurer, H.H., Meyer, M.R., 2017a. Pooled human liver preparations, HepaRG, or HepG2 cell lines for metabolism studies of new psychoactive substances? A study using MDMA, MDBD, butylone, MDPPP, MDPV, MDPB, 5-MAPB, and 5-API as examples. J. Pharm. Biomed. Anal. 143, 32–42.
Richter, L.H.J., Maurer, H.H., Meyer, M.R., 2017b. New psychoactive substances: studies on the metabolism of XLR-11, AB-PINACA, FUB-PB-22, 4-methoxy-alpha-PVP, 25-I-NBOMe, and meclonazepam using human liver preparations in comparison to primary human hepatocytes, and human urine. Toxicol. Lett. 280, 142–150.
Rochester, J.R., 2013. Bisphenol A and human health: a review of the literature. Reprod. Toxicol. 42, 132–155.
Rubin, B.S., 2011. Bisphenol A: an endocrine disruptor with widespread exposure and multiple effects. J. Steroid Biochem. Mol. Biol. 127, 27–34.
Schymanski, E.L., Jeon, J., Gulde, R., Fenner, K., Ruff, M., Singer, H.P., Hollender, J., 2014. Identifying small molecules via high resolution mass spectrometry: communicating confidence. Environ. Sci. Technol. 48, 2097–2098.
Silva, M.J., Slakman, A.R., Reidy, J.A., Preau Jr., J.L., Herbert, A.R., Samandar, E., Needham, L.L., Calafat, A.M., 2004. Analysis of human urine for fifteen phthalate metabolites using automated solid-phase extraction. J. Chromatogr. B Analyt. Technol. Biomed. Life Sci. 805, 161–167.
Söderholm, K.-J., Mariotti, A., 1999. Bis-Gma–based resins in dentistry: are they safe? J. Am. Dent. Assoc. 130, 201–209.
Sunnegardh-Gronberg, K., van Dijken, J.W., Funegard, U., Lindberg, A., Nilsson, M., 2009. Selection of dental materials and longevity of replaced restorations in Public Dental Health clinics in northern Sweden. J. Dent. 37, 673–678.
Tarumi, H., Imazoto, S., Narimatsu, M., Matsuo, M., Ebisu, S., 2000. Estrogenicity of fissure sealants and adhesive resins determined by reporter gene assay. J. Dent. Res. 79, 1838–1843.
United Nations Environment Programme, 2013. Minamata Convention on Mercury. Online available at. (Accessed December 2018). http://www.mercuryconvention.org.
Van Landuyt, K.L., Nawrot, T., Geebelen, B., De Munck, J., Snauwaert, J., Yoshihara, K., Scheers, H., Godderis, L., Hoet, P., Van Meerbeek, B., 2011. How much do resin-based dental materials release? A meta-analytical approach. Dent. Mater. 27, 723–747.
Vandenberg, L.N., Maffini, M.V., Sonnenschein, C., Rubin, B.S., Soto, A.M., 2009. Bisphenol-A and the great divide: a review of controversies in the field of endocrine disruption. Endocr. Rev. 30, 75–95.
Vervliet, P., de Nys, S., Boonen, I., Duca, R.C., Elskens, M., van Landuyt, K.L., Covaci, A., 2018a. Qualitative analysis of dental material ingredients, composite resins and sealants using liquid chromatography coupled to quadrupole time of flight mass spectrometry. J. Chromatogr. A 1576, 90–100.
Vervliet, P., Mortele, O., Gys, C., Degreef, M., Lanckmans, K., Maudens, K., Covaci, A., van Nuijs, A.L.N., Lai, F.Y., 2018b. Suspect and non-target screening workflows to investigate the in vitro and in vivo metabolism of the synthetic cannabinoid 5Cl-THJ-018. Drug Test. Anal.
World Health Organisation, 2011. Future use of materials for dental restoration. Geneva, Switzerland.
Xue, J., Wu, Q., Sakthivel, S., Pavithran, P.V., Vasukutty, J.R., Kannan, K., 2015. Urinary levels of endocrine-disrupting chemicals, including bisphenols, bisphenol A diglycidyl ethers, benzophenones, parabens, and triclosan in obese and non-obese Indian children. Environ. Res. 137, 120–128.
Zoeller, R.T., Brown, T.R., Doan, L.L., Gore, A.C., Skakkebaek, N.E., Soto, A.M., Woodruff, T.J., Vom Saal, F.S., 2012. Endocrine-disrupting chemicals and public health protection: a statement of principles from the Endocrine Society. Endocrinology 153, 4097–4110.